PAPER • **OPEN ACCESS**

Growth Characteristic of Microbubble in a Co-flowing Liquid in Microfluidic Chip

To cite this article: Lixia Sun *et al* 2019 *IOP Conf. Ser.: Earth Environ. Sci.* **295** 032007

Growth Characteristic of Microbubble in a Co-flowing Liquid in Microfluidic Chip

Lixia Sun[1,2], Mingxu Fan[2], Bo Xu[2,*], Huadong Yu[1,*], Yue Wang[2], Yufeng Zhang[2] and Peng Li[2]

[1]College of Mechanical and Electrical Engineering, Changchun University of Science and Technology, Changchun 130022, Jilin, China

[2]College of Mechanical Engineering, Beihua University, Jilin 132022, Jilin, China

*Corresponding author: 793487509@qq.com

*Corresponding author: Huadong2004@163.com

Abstract. Experiments of microbubble formation in a co-flowing liquid in polydimethylsiloxane (PDMS) microfluidic chip were developed. The experimental system was set up to investigate the effects of liquid flow rate, gas pressure, gas channel width and concentration of polyvinyl alcohol (PVA) solution on microbubble growth process. Three stages of the bubble growth process were first obtained through experiments. The control variable method was used to explore the growth characteristics of bubbles, such as the volume change rate, the contact angle, the ratio of length to width, and the centroid displacement. This study provides an empirical reference for the growth process of microbubbles in microfluidic chips, which helps to achieve precise control of microbubble volume and generation frequency.

1. Introduction

Microbubbles have many features that are not available in conventional bubbles, such as large specific surface area, slow rising speed[1,2], and high mass transferring efficiency[3]. Microbubbles are widely used in many fields such as biology, chemical industry and medical [4-5]. From the past to the present, many scholars engaged in fluid dynamics research are devoted to the study of the formation[6-7] and breakup[8-9] of microbubbles in microfluidic chip. According to the principle of bubble formation, the shape of the microchannel of the microfluidic chip is also different, such as co-flowing microchannel, T-junction microchannel and electrowetting method[10]. For different microchannel forms and bubble generation methods, scholars first provide theoretical support for bubble formation experiments from theoretical models and numerical simulations.

In the early days, experts thought that bubble growth in a microfluidic chip was staged, and the theoretical model according to the actual growth of the bubble is also divided into a one-stage model[11], two-stage model[12-15] and three-stage model[16-17]. Yu[18] et al. proposed a theoretical model of bubble formation and pointed out that bubble formation can be divided into three stages: the expansion stage, the elongation stage, and the pinch-off stage. W. B. Chen[19-20] used the interface element analysis method to establish a two-phase bubble non-spherical theoretical model. G. Biswas[21], et al. used a coupled level-set and volume-of-fluid (CLSVOF) method to simulated the rise and shape of two co-axial gas bubbles with same size in stagnant Newtonian liquid. L Dai[22], et al. numerically studied bubble emergence in a gas-liquid flow in a T-junction microchannel of 100 μm diameter.

Based on theoretical research, various microbubble formation experiments have also been carried out. Volkert van Steijn[23] et al. used a T-junction microfluidic device to study the bubble and droplet formation characteristics. D Caprini[24] et al. designed a T-junction device allowing for two simultaneous orthogonal views and the device application to bubble formation and break-up.

Although there are many methods for preparing microbubbles, most experiments only focus on the final formation of bubbles and ignore the growth process. This paper describes an experimental method for bubble formation in co-flowing liquid in PDMS microfluidic chip. The growth characteristics of bubbles in a co-flowing focusing environment was investigated, and the volume change rate, the ratio of length to width and the centroid displacement of the bubble are innovatively summarized.

2. Experimental

2.1 Experimental Setup

The PDMS microfluidic chip which was used for preparing microbubble has been designed, and the structure of the PDMS chip is shown in figure 1. All channels of the PDMS chip have a depth of 60 μm. The gas channel width is 60 μm, and the liquid channel width is 4 mm. The PDMS microfluidic chip contains a liquid inlet, a gas inlet, a bubble formation area, and a gas-liquid mixture outlet. PVA solution and nitrogen gas flow into the chip through the liquid inlet and the gas inlet respectively, and they converge at the bubble formation area to form bubbles.

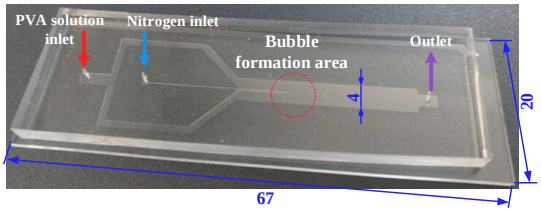

Figure 1. Structure of the PDMS chip

The schematic diagram of the experimental system is shown in figure 2. A syringe pump(704500, Harvard Apparatus) is used to regulate liquid flow rate; A relieve valve(YQD-4), a precision barometer(OMEGA PRG200-25) and a precision digital pressure gauge(YK-100) are used to adjust gas pressure in real time; The image acquisition system includes a microscope(Olympus CX21) and a high-speed camera(Phantom v12.1, 100w fps) which are used for collecting image information during bubble growth.

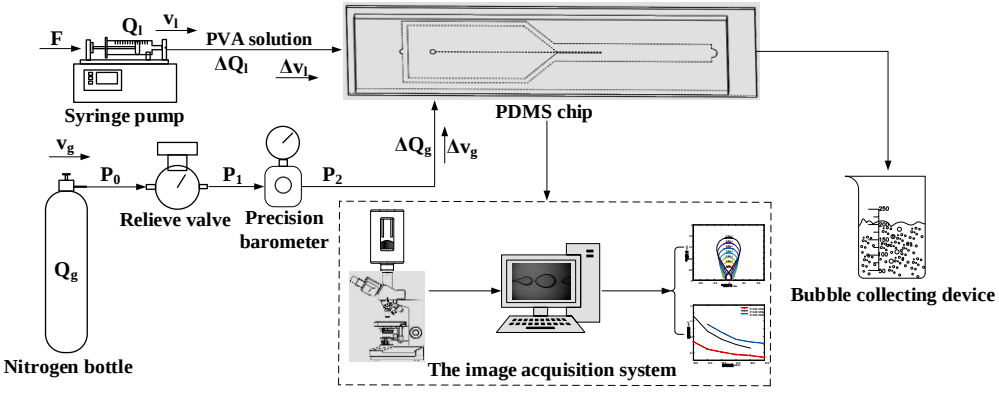

Figure 2. Schematic diagram of the experimental system

2.2 Experimental Process

Experimental parameters and independent variable ranges should be bound before the microbubble formation experiment. The adjustment range of the gas pressure is 30 kPa to 70 kPa, and the gradient is 5 kPa; The range of liquid flow rate is 200 mLh^{-1} to 450 mLh^{-1}, and the gradient is 50 mLh^{-1}; Other experimental parameters and their values are shown in table 1. During the experiment, the high-speed microscopic observation system was used to collect the bubble formation images under various working conditions. Photoshop, Image Pro Plus 6.0 and MATLAB are used to obtain the volume of bubble, the contact angle and other data of bubbles.

Table 1. Experimental parameters and their values

Parameter	Value
Gas channel width d_g [μm]	60/100
Liquid channel width d_L [mm]	4
Concentration of PVA solution	2%/3%
Liquid dynamic viscosity μ_L [Pa s]	4.9×10-3
Liquid density ρ_L [kg m^{-3}]	1002
Gas density ρ_g [kg m^{-3}]	1.25
Surface tension coefficient σ [N m^{-1}]	0.053

3. Results and Discussion

3.1 Microbubble Growth Process

During the experiment, the liquid channel width is set to 60 μm, and the concentration of PVA solution is 2%. The liquid flow rate is 200 mLh^{-1} and the gas pressure is 30 kPa. The image of bubble growth process obtained by high-speed microscopic observation system is shown in figure 3. It can be seen from the images that the microbubble growth process can be divided into three stages: an expansion stage, an axial stretching stage, and a necking detachment stage.

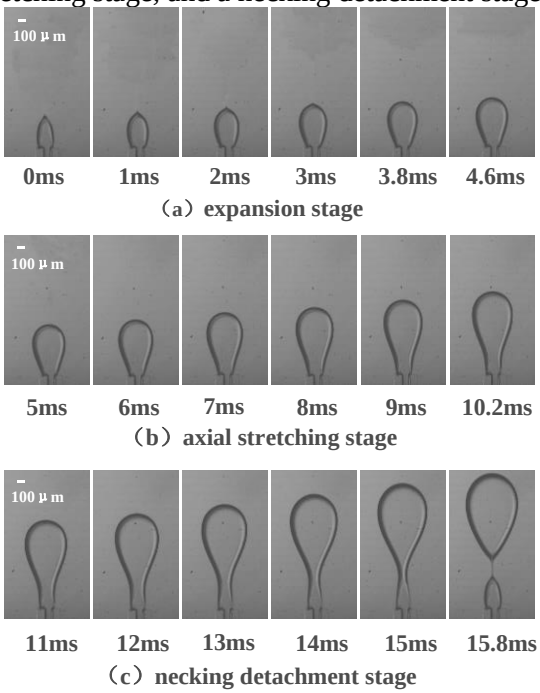

Figure 3. Microbubble growth process

3.2 Volume Change Rate

During the experiment, the PDMS chip with a gas channel width of 60 μm is selected, the concentration of PVA solution is 3%. The gas pressure is 50 kPa, 60 kPa and 65 kPa respectively, the liquid flow rate is 300 mLh^{-1} and 400 mLh^{-1} respectively. The volume of a bubble at each moment in a growth cycle under different working conditions is measured. The curve of bubble volume with time is shown in figure 4.

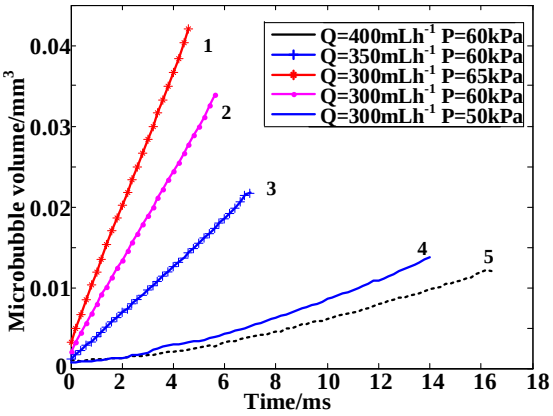

Figure 4. Curve of bubble volume with time under different working conditions

As is evident in figure 4, the slope of the curve represents the volume change rate of the bubble. By control variable method, it can be known by comparing the slopes of the curves that the volume change rate of the bubble increases with gas pressure increases and decreases with liquid flow rate increases. The slopes of curve 1 and curve 2 are large, and the bubble volume changes linearly with time. However, the slopes of curve 4 and curve 5 are small, and the bubble grows slowly in the early stage. This may be because the bubble needs to overcome a large surface tension in the early growth stage, and the gas velocity is low, resulting in a small volume change rate.

3.3 Contact Angle

The angle between the bubble and the end face of the stomata is defined as the contact angle, as shown in figure 5. In the figure, θ represents the contact angle.

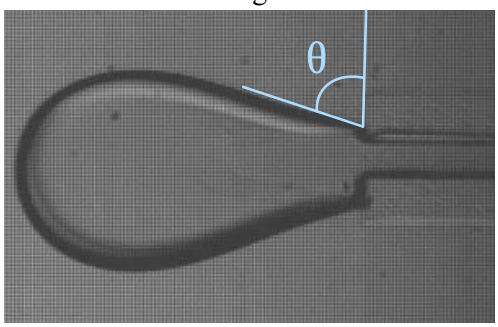

Figure 5. Microbubble contact angle

This experiment uses the control variable method to explore the influence of environmental factors on the contact angle. The first working condition: gas channel width is 60 μm, concentration of PVA solution is 3%, liquid flow rate is 300 mLh^{-1} and gas pressure is 60 kPa. The second working condition: gas channel width is 100 μm, concentration of PVA solution is 2%, liquid flow rate is 250 mLh^{-1} and gas pressure is 65 kPa. In each group of control experiments, three variables were controlled to remain constant and the fourth variable was changed. The curve of bubble contact angle with time is shown in figure 6.

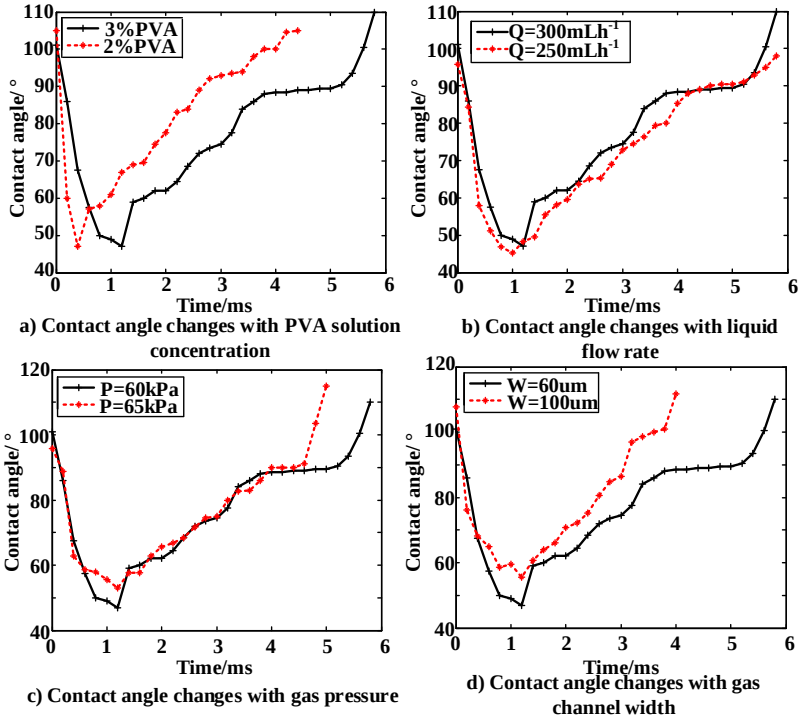

Figure 6. Curve of contact angle with time under different working conditions

As is observed in Figure 6, contact angle greater than 90° at the beginning and end of bubble growth process. The contact angle has the same change rule under different working conditions, that is, decrease firstly and then increase. Contact angle reflects the degree of wetting of the PDMS chip, and the smaller the contact angle, the higher the degree of wetting. The change rule of contact angle is also related to the hydrophobicity and surface roughness of the PDMS chip.

3.4 Ratio of Length to Width and the Centroid Displacement

In order to better describe the contour change rule of the bubble during the growth process, the concept of ratio of length to width and the centroid displacement is introduced, as shown in figure 7.

In the figure, L is the maximum length of the bubble along the gas channel, W is the maximum width of the bubble along the direction perpendicular to the gas channel. An intersection point A which between the length and width of the bubble is defined as the centroid.

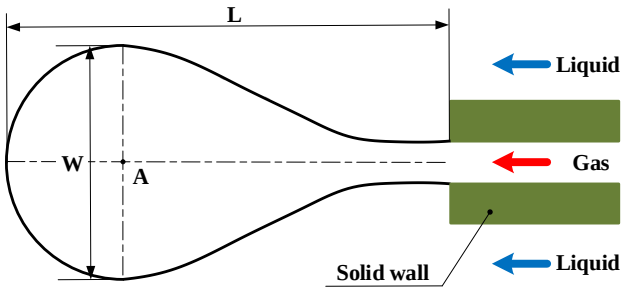

Figure 7. The length, width and centroid of bubble

During the experiment, the gas channel width is set to 60 μm, concentration of PVA solution is 2%, gas pressure is 40 kPa, 50 kPa, 60 kPa and 70 kPa respectively, liquid flow rate is 200 mLh^{-1}, 250 mLh^{-1}, 300 mLh^{-1}, 350 mLh^{-1} respectively. The length, width and centroid coordinates of the bubble at each moment throughout the growth cycle under different conditions were obtained, as shown in figure 8 and figure 9.

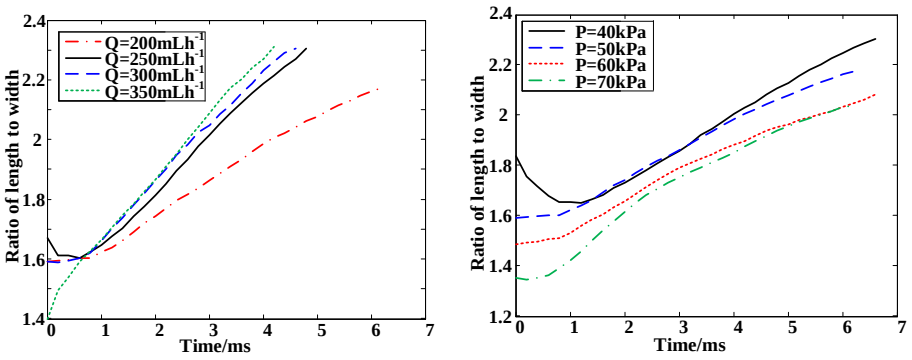

a) b)

Figure 8. Ratio of length to width changes with time under different working conditions

In figure 8 a), gas pressure is 50 kPa. It can be seen from figure 8 a) that the ratio of length to width grows slowly in the early stages of bubble growth, which indicates that the size of the length and width of the bubble increases at the same time, and the increase rate is similar. In the middle and late stages of bubble growth, the ratio of length to width increases almost linearly, which indicates that the growth rate of the bubble along the length direction is significantly greater than that in the width direction at this stage, and the bubble is elongated. It can be known from the slope of the curve gradually increasing that the change rate of the ratio of length to width increases with the liquid flow rate increases. This may be because the liquid pulling force of the bubble increases with the liquid flow rate increases, which causing the bubble to grow along the length direction. Figure 8 b) depicts the change rate of the ratio of length to width with time when the liquid flow rate is 200 mLh^{-1}. It can be seen from the figure that the change rate of the ratio of length to width decreases with the gas pressure increases. This may be because the gas pressure which increases inside the bubble will prevent the bubble from shrinking in the width direction.

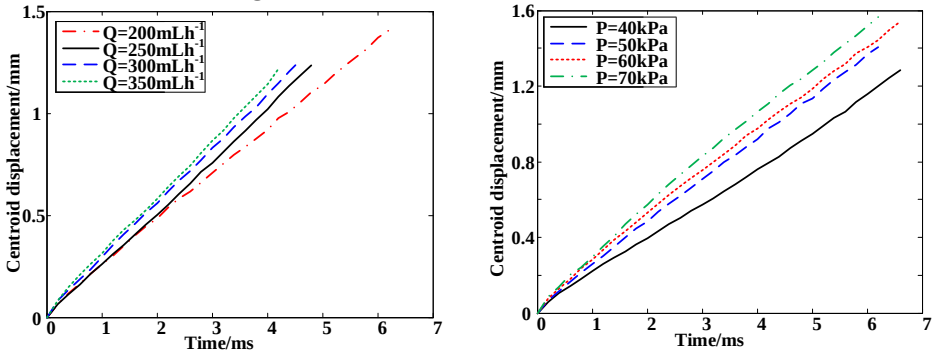

a) b)

Figure 9. Centroid displacement changes with time under different working conditions

Figure 9 a) shows the change rate of centroid displacement with time under different liquid flow rates when the gas pressure is 50 kPa. It is easy to see from the figure that the centroid displacement increases linearly throughout the bubble growth cycle, and the slope of the line represents the moving velocity of the centroid. Through the comparison between the curves, it can be found that the moving velocity of the centroid increases with the liquid flow rate increases, which indicates the moving velocity of the centroid is positively correlated with the liquid flow rate. In figure 9 b), the liquid flow rate is 200 mLh^{-1}. As is evident in figure 9 b), the centroid displacement increases linearly under different gas pressures. The moving velocity of the centroid increases with the gas pressure increases, which shows the moving velocity of the centroid is positively correlated with the gas pressure.

4. Conclusions

In the present study, growth characteristic of microbubble in a co-flowing liquid in microfluidic chip was investigated experimentally. Four important characteristics: Volume change rate, Contact angle,

Ratio of length to width and Centroid displacement have been focused on and studied in details. According to the research content of this paper, there are following conclusions:

(1) The volume change rate of the bubble increases with gas pressure increases and decreases with liquid flow rate increases, and the bubble volume changes linearly with time. However, the experimental results also show that the volume of the bubble is greatly affected by the surface tension.

(2) The contact angle decreases first and then increases during bubble growth process under different environmental conditions. The change rule of contact angle is related to the hydrophobicity and surface roughness of the PDMS chip. Moreover, the increasing contact angle also indicates that the bubble is gradually detached.

(3) The ratio of length to width increases with time under different liquid flow rates or gas pressures, which indicates that the ratio of length to width is most affected by liquid flow rate. When liquid flow rate increase, the liquid pulling force also increase, and the liquid pulling force is the main reason for the increase in the ratio of length to width.

(4) The centroid displacement increases with time linearly under different working conditions, which illustrates that the growth velocity of the bubble is uniform, and mainly reflected in the growth velocity of the bubble along the length direction.

Results of the present study vastly enhance our understanding of the growth process of single bubble in co-flowing liquid. The results of this study provide a reference for the growth of microbubbles in different microchannels, and they can help to achieve precise control of microbubble volume and generation frequency in microfluidic chip. Due to the slow floating rate and high mass transfer efficiency of microbubble, the next research plan is to use microfluidic chip to prepare microbubbles with controllable volume and generation frequency, and ozone can be injected into microbubbles to oxidize organic pollutants in water.

Acknowledgment
This work was supported by Science and Technology Department of Jilin Province [grant number 20190302039GX].

References

[1] YANG L, LIAO C, ZHU Y, CHEN H and JIN Q 2012 *Chem. Indus. Eng. Prog*. 6, 1333.
[2] Zhou L V, Shan-Chang C, Ting C and Jian W 2014 *Guangzhou. Chem. Indus*. 42, 122.
[3] Takahashi M, Kawamura T, Yamamoto Y, Ohnari H, Himuro S and Shakutsui H 2016 *J. Phys. Chem*. 107, 2171.
[4] Garstecki P 2005 *Bull. Pol. Acad. Sci. Tech. Sci.* 53, 361.
[5] Zhu P, Tang X and Wang L 2016 *Microflu. Nanoflu*. 20, 1.
[6] Tice J D, Lyon A D and Ismagilov R F 2004 *Anal. Chim. Acta*. 507, 73.
[7] Xu J H, Luo G S, Li S W, Li S W and Chen G G 2005 *Lab Chip*. 6, 131.
[8] Dai C, Fang S, Wu Y, Wu X, Zhao M and Zou C 2017 *Colloids Surf. A*, 535, 130.
[9] Wang X, Zhu C, Fu T and Ma Y 2015 *AIChE J*. 61,1081.
[10] Teh S Y, Lin R, Hung L H, Hung L H and Lee A P 2008 *Lab Chip*, 8, 198.
[11] Orzechowski Z 1990 *Państwowe Wydawnictwo Naukowe*.
[12] Tsuge H and Hibino S 1978 *J Chem Eng Jpn*. 11, 173.
[13] Miyahara T, Matsuba Y and Takahashi T 1983 *Inter Chem Eng*, 524.
[14] Miyahara T and Takahashi T 1984 *J Chem Eng Jpn*, 17, 597.
[15] Gaddis E S and Vogelpohl A 1986 *Chem Eng Sci*, 41, 97.
[16] Kupferberg A and Jameson G J 1969 *Trans Instit Chem Eng*, 47, 241.
[17] Tsuge H and Hibino S 1983 *Chem Eng Commun*, 22, 63.
[18] Yu X, Wang Y, Huang C and Du T 2015 *J. Phys*. 656.
[19] Chen W B and Tan R B H 2003 *AIChE J*. 49, 1964.
[20] Chen W B and Tan R B H 2002 *J. Chem. Eng. Jpn*. 35, 952.
[21] Chakraborty I, Biswas G and Ghoshdastidar P S 2013 *Int. J. Heat Mass Transfer*, 58, 240.

[22] Dai L, Cai W and Xin F 2010 *Chem. Eng. Technol*, 32, 1984.
[23] Van S V, Kleijn C R and Kreutzer M T 2010 *Lab Chip*. 10, 2513.
[24] Caprini D, Sinibaldi G, Marino L and Casciola C M 2018 *Microflu. Nanoflu.* 22, 85.